

The New F_L Measurement from HERA and the Dipole Model

Carlo Ewerz^{a,b,1}, Andreas von Manteuffel^{c,d,2},
Otto Nachtmann^{a,3}, André Schöning^{e,4}

^a *Institut für Theoretische Physik, Universität Heidelberg
Philosophenweg 16, D-69120 Heidelberg, Germany*

^b *ExtreMe Matter Institute EMMI, GSI Helmholtzzentrum für Schwerionenforschung
Planckstraße 1, D-64291 Darmstadt, Germany*

^c *Institut für Theoretische Physik, Universität Zürich
Winterthurerstr. 190, CH-8057 Zürich, Switzerland*

^d *Institut für Physik (THEP), Johannes-Gutenberg-Universität
D-55099 Mainz, Germany*

^e *Physikalisches Institut, Universität Heidelberg
Philosophenweg 12, D-69120 Heidelberg, Germany*

Abstract

From the new measurement of F_L at HERA we derive fixed- Q^2 averages $\langle F_L/F_2 \rangle$. We compare these with bounds which are rigorous in the framework of the standard dipole picture. The bounds are sharpened by including information on the charm structure function $F_2^{(c)}$. Within the experimental errors the bounds are respected by the data. But for $3.5 \text{ GeV}^2 \leq Q^2 \leq 20 \text{ GeV}^2$ the central values of the data are close to and in some cases even above the bounds. Data on F_L/F_2 significantly exceeding the bounds would rule out the standard dipole picture at these kinematic points. We discuss, furthermore, how data respecting the bounds but coming close to them can give information on questions like colour transparency, saturation and the dependencies of the dipole-proton cross section on the energy and the dipole size.

¹ email: C.Ewerz@thphys.uni-heidelberg.de

² email: manteuffel@uni-mainz.de

³ email: O.Nachtmann@thphys.uni-heidelberg.de

⁴ email: schoening@physi.uni-heidelberg.de

1 Introduction

Recently new results for the structure functions F_L and F_2 of deep inelastic electron- and positron-proton scattering (DIS) have been published by the H1 Collaboration [1]. In this note we compare these results with predictions of the popular colour-dipole model of DIS. That is, we investigate if the data respect certain bounds for the ratios of structure functions. These bounds are rigorous predictions of the dipole model and rely only on the non-negativity of the dipole-proton cross section.

The kinematics of $e^\pm p$ scattering is well known, see for instance [1, 2]. The reaction is

$$e^\pm(k) + p(p) \longrightarrow e^\pm(k') + X(p') \quad (1)$$

and we use the variables

$$\begin{aligned} q &= k - k' = p' - p, & Q^2 &= -q^2, \\ W^2 &= (p + q)^2, & x &= \frac{Q^2}{2pq} = \frac{Q^2}{W^2 + Q^2 - m_p^2}. \end{aligned} \quad (2)$$

The measured structure functions F_2 and F_L are related to the cross sections σ_T and σ_L for absorption of transversely or longitudinally polarised virtual photons by

$$\begin{aligned} F_2(x, Q^2) &= \frac{Q^2}{4\pi^2\alpha_{\text{em}}} (1 - x) [\sigma_T(x, Q^2) + \sigma_L(x, Q^2)], \\ F_L(x, Q^2) &= \frac{Q^2}{4\pi^2\alpha_{\text{em}}} (1 - x) \sigma_L(x, Q^2). \end{aligned} \quad (3)$$

Here Hand's convention [3] for the virtual-photon flux factor is used and terms of order m_p^2/W^2 are neglected. For low to moderate values of Q^2 the dipole picture for DIS [4, 5, 6] is frequently used to describe the data. For various applications of the dipole model see for instance [7]-[27]. In [28, 29] this dipole picture was thoroughly examined using functional methods of quantum field theory. In particular, the assumptions were spelled out which one has to make in order to arrive at the standard dipole-model formulae for σ_T and σ_L or, equivalently, F_2 and F_L ,

$$\begin{aligned} F_2(x, Q^2) &= \frac{Q^2}{4\pi^2\alpha_{\text{em}}} (1 - x) \sum_q \int d^2r \left[w_T^{(q)}(r, Q^2) + w_L^{(q)}(r, Q^2) \right] \hat{\sigma}^{(q)}(r, \xi), \\ F_L(x, Q^2) &= \frac{Q^2}{4\pi^2\alpha_{\text{em}}} (1 - x) \sum_q \int d^2r w_L^{(q)}(r, Q^2) \hat{\sigma}^{(q)}(r, \xi), \end{aligned} \quad (4)$$

see section 6 of [29]. In (4) $w_{T,L}^{(q)}$ are the probability densities for the virtual photon γ^* splitting into a quark-antiquark pair of flavour q and transverse separation r . Their standard expressions are given in Appendix A. An integration over the quark's longitudinal momentum is performed. The cross section for the $q\bar{q}$ pair scattering on the proton is denoted by $\hat{\sigma}^{(q)}(r, \xi)$. This cross section depends on r and an energy variable ξ the choice of which is left open here. In [28, 29, 30, 31, 32] it was argued that the correct variable to choose is $\xi = W$. However, in the literature the energy variable used most frequently in the dipole cross section is $\xi = x$.

In the standard dipole model formulae (4) the densities $w_{T,L}^{(q)}$ are known (see Appendix A) but the dipole-proton cross sections $\hat{\sigma}^{(q)}$ have to be taken from a model. In the following we shall only use that they have to be non-negative,

$$\hat{\sigma}^{(q)}(r, \xi) \geq 0. \quad (5)$$

This alone allows to derive a non-trivial upper bound, valid in any dipole model, on the ratio

$$R(x, Q^2) = \frac{\sigma_L(x, Q^2)}{\sigma_T(x, Q^2)} \quad (6)$$

see [29, 30]. Equivalently, one can obtain a non-trivial upper bound on the ratio

$$\frac{F_L(x, Q^2)}{F_2(x, Q^2)} = \frac{R(x, Q^2)}{1 + R(x, Q^2)}. \quad (7)$$

This bound can be substantially improved if information on the charm structure function $F_2^{(c)}(x, Q^2)$ is included [31]. There is then an allowed domain, again valid in any dipole model, for the two-dimensional vector

$$\vec{V}(x, Q^2) = \begin{pmatrix} F_L(x, Q^2)/F_2(x, Q^2) \\ F_2^{(c)}(x, Q^2)/F_2(x, Q^2) \end{pmatrix}. \quad (8)$$

It is the purpose of this note to confront the dipole-model bounds on F_L/F_2 and on the vector $\vec{V}(x, Q^2)$ with the new HERA results [1]. This is done in section 2. In section 3 we discuss the results, and we give a summary in section 4.

2 The dipole-model bounds and the data

We discuss first the bound for the ratio F_L/F_2 of (7). For this we define

$$g(Q, r, m_q) = \frac{w_L^{(q)}(r, Q^2)}{w_T^{(q)}(r, Q^2) + w_L^{(q)}(r, Q^2)}, \quad (9)$$

where m_q is the mass of the quark q . For the case of massless quarks, $m_q = 0$, figure 1 shows $\frac{1}{\alpha_{\text{em}} Q_q^2}(w_T^{(q)} + w_L^{(q)})(r, Q^2)$ and $g(Q, r, 0)$ as functions of r for three different values of $Q = \sqrt{Q^2}$ (compare figure 10 of [29] for a similar plot of the function $(w_L^{(q)}/w_T^{(q)})(r, Q^2)$). Note that $(w_T^{(q)} + w_L^{(q)})(r, Q^2)$ is monotonously decreasing with r . Its behaviour for small and large r is as follows for $m_q = 0$:

$$\begin{aligned} (w_T^{(q)} + w_L^{(q)})(r, Q^2) &\propto \frac{1}{r^2} & \text{for } r \rightarrow 0, \\ (w_T^{(q)} + w_L^{(q)})(r, Q^2) &\propto \frac{1}{r^4} & \text{for } r \rightarrow \infty. \end{aligned} \quad (10)$$

For a derivation of these results and for the case $m_q \neq 0$ see appendix A of [32]. For massless quarks the function g depends only on the dimensionless variable

$$z = Qr, \quad (11)$$

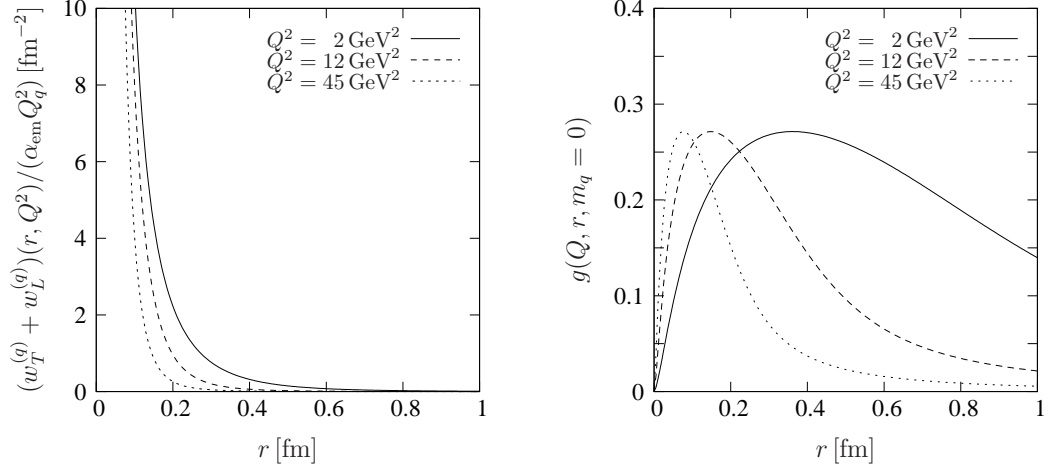


Figure 1: The functions $\frac{1}{\alpha_{\text{em}} Q_q^2} (w_T^{(q)} + w_L^{(q)})(r, Q^2)$ (left) and $g(Q, r, m_q)$ (right) versus r , both for three fixed values of Q^2 and for quark mass $m_q = 0$; see (4) and (9).

such that we can write

$$\tilde{g}(z) = g(Q, r, 0). \quad (12)$$

The function $\tilde{g}(z)$ has a maximum at

$$z_m = 2.5915 \quad (13)$$

with

$$\tilde{g}(z_m) = 0.27139. \quad (14)$$

It was shown in [31] that

$$g(Q, r, m_q) \leq \tilde{g}(z_m) \quad (15)$$

for all $Q \geq 0$, $r \geq 0$ and $m_q \geq 0$. Using then (5) the dipole-model formulae (4) lead to the bound

$$\frac{F_L(x, Q^2)}{F_2(x, Q^2)} \leq \tilde{g}(z_m) = 0.27139. \quad (16)$$

We note that the bound (16) for F_L/F_2 is equivalent to the bound for R (6) derived in [30, 31],

$$R(x, Q^2) \leq \frac{\tilde{g}(z_m)}{1 - \tilde{g}(z_m)} = 0.37248. \quad (17)$$

Data for F_L and F_2 at the same kinematic points are presented in [1] for Q^2 values ranging from 1.5 to 45 GeV^2 . The data for the same Q^2 value span a small range of x and this range varies strongly with Q^2 ; see figure 12 of [1]. On the other hand, for all Q^2 bins the data are inside a narrow W interval

$$167 \text{ GeV} - 232 \text{ GeV} \quad (18)$$

with a mean value of about $W_0 = 200 \text{ GeV}$. Therefore, in the following we find it more convenient to consider F_L and F_2 as functions of W and Q^2 instead of x and Q^2 .

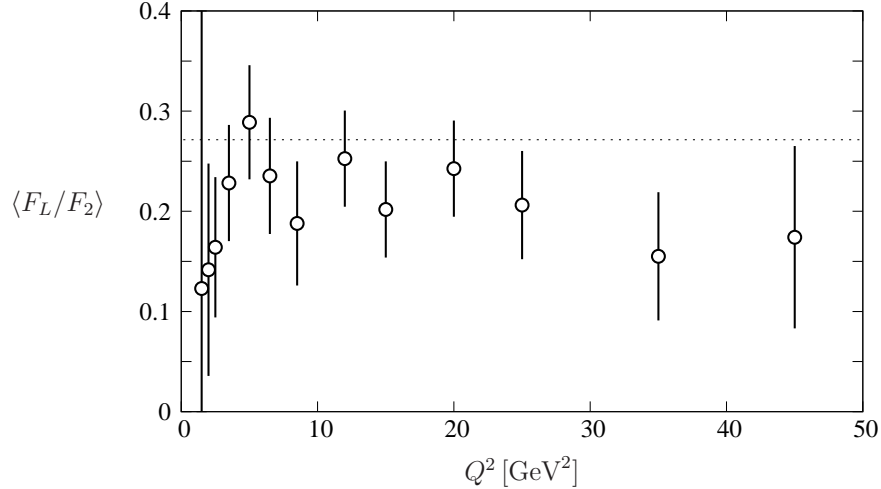


Figure 2: The data for the fixed- Q^2 averages $\langle F_L/F_2 \rangle$ confronted with the dipole-model upper bound (16) represented by the dotted line. The data are extracted from [1].

Since we do not expect any large variation of the ratio $F_L(W, Q^2)/F_2(W, Q^2)$ for fixed Q^2 within the W interval (18) of the measurement we have averaged the H1 data [1] for given Q^2 . Error weighted averages $\langle F_L(W, Q^2)/F_2(W, Q^2) \rangle$ are calculated taking into account the total uncorrelated and correlated experimental uncertainties. The averages are confronted with the bound (16) in figure 2.

We note firstly, that electromagnetic gauge invariance requires

$$\frac{F_L(W, Q^2)}{F_2(W, Q^2)} \longrightarrow 0 \quad (19)$$

for $Q^2 \rightarrow 0$ at fixed W . The data indicate, indeed, a decrease of F_L/F_2 for small Q^2 . Fitting F_L/F_2 with a constant value, as done in [1], does not seem very plausible physically, in view of (19).

The second point to note is that the data in figure 2 are rather close to the upper bound (16) from the dipole model, especially so for

$$3.5 \text{ GeV}^2 \leq Q^2 \leq 20 \text{ GeV}^2. \quad (20)$$

The bound (16) on F_L/F_2 can be improved if one takes into account that there is a non-vanishing contribution from charm quarks to F_L and F_2 , see [31]. Specifically, considering massless u, d and s quarks, a massive c quark and neglecting b quarks we can derive certain allowed domains for the vector $\vec{V}(x, Q^2)$ (8) from the dipole model. Again these domains depend only on the known photon densities $w_{T,L}^{(q)}$, see (28)-(31), and on the non-negativity of the cross sections $\hat{\sigma}^{(q)}$, see (5). That is, for any dipole model with the standard photon probability densities $w_{T,L}^{(q)}$ the vector $\vec{V}(x, Q^2)$ must be inside the appropriate allowed domain for the given Q^2 value. A detailed description of how these domains are obtained has been given in [31]. The allowed domains can be understood as correlated bounds for the ratios F_L/F_2 and $F_2^{(c)}/F_2$. More precisely,

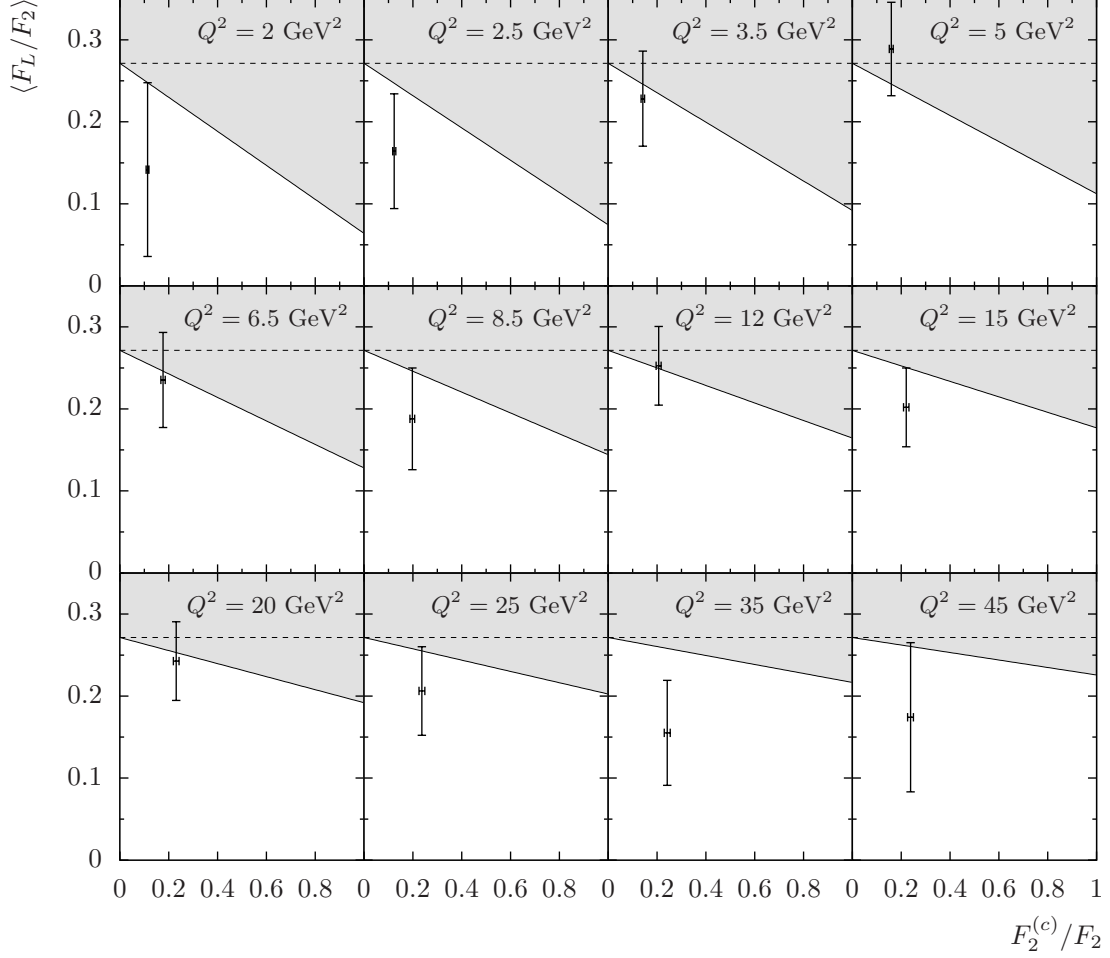


Figure 3: The allowed domains and the data for $\langle F_L/F_2 \rangle$ versus $F_2^{(c)}/F_2$ for $Q^2 = 2 \text{ GeV}^2$ to $Q^2 = 45 \text{ GeV}^2$. In the dipole model, the shaded areas are excluded by the correlated bounds for F_L/F_2 and $F_2^{(c)}/F_2$. The dotted line is the bound (16) on F_L/F_2 only.

one obtains for any given x and Q^2 an upper bound on F_L/F_2 which depends on the value of $F_2^{(c)}/F_2$ at the same kinematic point.

In figure 3 we show these allowed domains and the corresponding data. The bounds are calculated for a charm quark mass of $m_c = 1.23 \text{ GeV}$. For each data point the corresponding ratio $F_2^{(c)}/F_2$ is obtained using NLO QCD calculations provided by the OPENQCDRAD package [33], again with a charm pole mass of $m_c = 1.23 \text{ GeV}$. For this calculation the JR09FFNNLO parametrisation [34] of the proton parton density functions was used, which was found to describe preliminary HERA charm data [35] very well within the experimental correlated uncertainties of typically 3-9%. Here and in the following we do not consider the data point at $Q^2 = 1.5 \text{ GeV}^2$ from [1] as it has an exceedingly large error.

The significance of the data points in relation to the bound can be seen more clearly

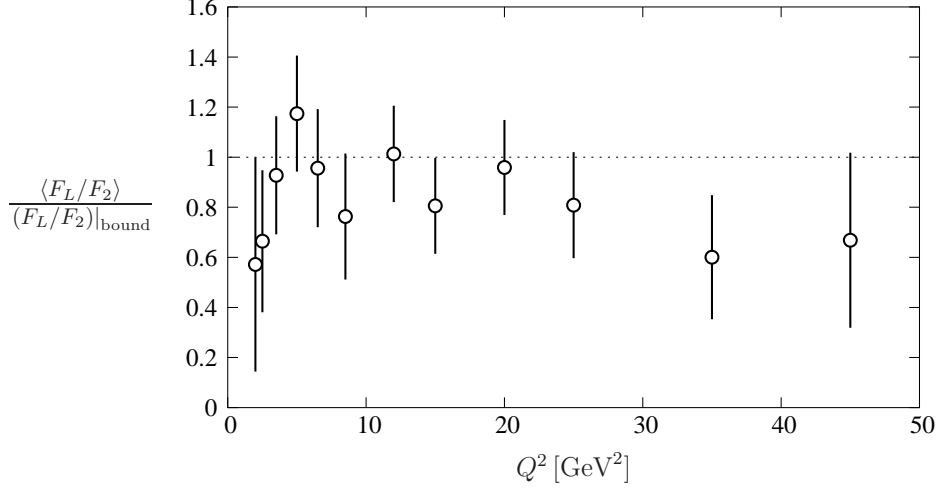


Figure 4: The ratio $\langle F_L/F_2 \rangle / (F_L/F_2)|_{\text{bound}}$, see (21), where the bound on F_L/F_2 results from taking into account the value of $F_2^{(c)}/F_2$ at the kinematical point of each data point.

from the quantity

$$\frac{\langle F_L/F_2 \rangle}{(F_L/F_2)|_{\text{bound}}} \quad (21)$$

which we plot in figure 4. For this figure the bound $(F_L/F_2)|_{\text{bound}}$ for each data point is extracted from figure 3 taking into account the corresponding value of $F_2^{(c)}/F_2$ at that kinematical point.

3 Discussion

We see from figures 2-4 that the data for $\langle F_L/F_2 \rangle$ as derived from [1] come very close to the bounds which result from the dipole picture. We now discuss the meaning of this observation from the points of view of both, a dipole-model enthusiast, and a dipole-model sceptic, respectively.

Dipole-model enthusiast's view

The dipole-model enthusiast will say that within the errors of the data the bounds are respected. Furthermore, he can use the data to give qualitative arguments concerning the behaviour of the dipole-proton cross sections for small and large radii r . Let us assume power behaviour of $\hat{\sigma}^{(q)}(r, \xi)$ for $r \rightarrow 0$ and $r \rightarrow \infty$,

$$\begin{aligned} \hat{\sigma}^{(q)}(r, \xi) &\propto r^a & \text{for } r \rightarrow 0, \\ \hat{\sigma}^{(q)}(r, \xi) &\propto r^{2-b} & \text{for } r \rightarrow \infty. \end{aligned} \quad (22)$$

Taking into account (10) we find that the integrals for F_2 and F_L in (4) are convergent if

$$a > 0 \quad \text{and} \quad b > 0. \quad (23)$$

Of course, with the usual assumptions of colour transparency for small r , implying $a = 2$, and of saturation for the dipole-proton cross sections for large r , implying $b = 2$, the requirements (23) are satisfied. From the experimental findings of figures 2 to 4 we can now give qualitative arguments based on the data, that the exponents a and b in (22) cannot be too small. Indeed, for a small value of a the cross sections $\hat{\sigma}^{(q)}(r, \xi)$ would decrease only slowly for $r \rightarrow 0$ and this region of small r would contribute significantly in the integrals (4). But, as we see from the second plot in figure 1, the function $g(Q, r, 0)$ is small there and this would lead to a small value for F_L/F_2 , much below the bound (16), contrary to what is seen in the data. A similar argument applies to the exponent b in (23), considering the large r behaviour of $g(Q, r, 0)$ in figure 1. Thus, the dipole-model enthusiast may hope that with more data it may even be possible to determine the exponents a and b from the data on F_L/F_2 directly without making model assumptions for $\hat{\sigma}^{(q)}(r, \xi)$.

Dipole-model sceptic's view

Let us now go over to the point of view of the dipole-model sceptic. He will note that some central values of the data for F_L/F_2 in figure 3 are, in fact, *above* the corresponding bound. If any of the measured points with $\langle F_L/F_2 \rangle > (F_L/F_2)|_{\text{bound}}$ is confirmed, with corresponding small error, by further experiments then, as a clear consequence, the standard dipole picture would not be valid at this kinematic point. But what would be the consequences if the bound for F_L/F_2 is not *violated* but *saturated*?

For the sake of the argument we shall now for a moment *assume* that the bound for F_L/F_2 is reached in the Q^2 range (20). Clearly, this is not incompatible with the data, see figures 3 and 4. The consequence is that the dipole-proton cross sections $\hat{\sigma}^{(q)}(r, \xi)$ in (4) should only contribute at that particular r values where the functions $g(Q, r, 0)$ and $g(Q, r, m_c)$ of (9) have their maximum. This is for both functions the case for

$$r \approx \frac{0.51 \text{ fm}}{\sqrt{Q^2/\text{GeV}^2}}. \quad (24)$$

We see this for $g(Q, r, 0)$ from the second plot in figure 1 and this also holds for $g(Q, r, m_c)$. Thus, the cross sections $\hat{\sigma}^{(q)}(r, \xi)$ should be strongly peaked at these r values for the whole Q^2 interval (20), something like a δ function

$$\hat{\sigma}^{(q)}(r, \xi) \approx \delta\left(r - \frac{0.51}{Q}\right) \quad (r \text{ in fm, } Q \text{ in GeV}). \quad (25)$$

The corresponding r values range from 0.27 fm for $Q^2 = 3.5 \text{ GeV}^2$ to 0.11 fm for $Q^2 = 20 \text{ GeV}^2$. With increasing Q the position of the delta function peak in (25) moves to smaller r values. As we have argued at length in [28, 29, 32], the correct energy variable in the dipole-proton cross section $\hat{\sigma}^{(q)}(r, \xi)$ is $\xi = W$. Since the data on F_L/F_2 is essentially at one value of $W \approx W_0 = 200 \text{ GeV}$ (more precisely, in the narrow range (18) around W_0) we get from (25) a Q^2 dependence in $\hat{\sigma}^{(q)}(r, W_0)$ which should *not* be there. The conclusion is that a saturation of the bound on F_L/F_2 in a whole Q^2 interval as in (20) is incompatible with the dipole model and the dipole-proton cross sections having the correct functional dependence $\hat{\sigma}^{(q)}(r, W)$.

With the – incorrect – choice of energy variable $\xi = x$ in $\hat{\sigma}^{(q)}(r, \xi)$ we get the following. Since the data on F_L/F_2 is essentially at $W = W_0$ (namely in the narrow range (18) around W_0), we have from (2)

$$x \simeq \frac{Q^2}{W_0^2}, \quad Q \simeq \sqrt{x} W_0. \quad (26)$$

Inserting this in (25) gives

$$\hat{\sigma}^{(q)}(r, x) \approx \delta \left(r - \frac{0.51}{\sqrt{x} W_0} \right) \quad (r \text{ in fm, } W_0 \text{ in GeV}). \quad (27)$$

Thus, there is in this case no immediate conflict with the functional dependence $\hat{\sigma}^{(q)}(r, x)$. But we note that as x *decreases* the peak of the cross section $\hat{\sigma}^{(q)}(r, x)$ in (25) shifts to *larger* values of r . This is in contrast to what one finds in popular dipole models, like the one invented by Golec-Biernat and Wüsthoff [7]. There, one assumes a dipole-proton cross section saturating at large r with an x -dependent saturation scale. But in that model for *decreasing* values of x the cross section $\hat{\sigma}^{(q)}(r, x)$ moves to *smaller* values of r , see figure 2 of [7]. This is in contradiction to what we found above in (27).

The dipole-model sceptic could, furthermore, argue as follows. Since the bounds explored in the present paper are just more or less satisfied by the data it will certainly pay to explore further rigorous bounds which can be constructed using the methods of [31]. One could, for instance, consider correlated bounds on F_L/F_2 at different Q^2 values. It remains to be explored if the dipole model survives such extended tests.

4 Summary

In this paper we have compared the recent data on F_L/F_2 – to be precise: their fixed- Q^2 averages – with rigorous bounds derived in the framework of the dipole model. Within the experimental errors the bounds are satisfied. But the data is surprisingly close to the bounds for $3.5 \text{ GeV}^2 \leq Q^2 \leq 20 \text{ GeV}^2$. We have discussed the meaning of these findings from the points of view of both, the dipole-model enthusiast and the sceptic. The enthusiast will have to admit that the sceptic’s arguments could give problems to the dipole picture if the central values of the data are confirmed with small errors by further experiments. The sceptic will have to concede that, given the errors of the data, δ functions for the cross sections $\hat{\sigma}^{(q)}(r, \xi)$ as in (25) and (27) are not really necessary and that the widths of the distributions compatible with the data have to be explored. Thus, given the present data, we must leave it to the reader if he will join the camp of the enthusiast or that of the sceptic. More data with small errors would be needed to decide the issue. In any case we hope to have demonstrated in our paper that measurements of F_L/F_2 give very valuable information on the dipole picture, its validity, and potentially on questions like colour transparency and saturation of the dipole-proton cross section. Thus, programs for future electron- and positron-proton scattering experiments (see for instance [36], [37]) certainly should foresee F_L measurements as an important item on the list of physics topics.

Acknowledgements

We are grateful to Sascha Glazov for providing data tables and information on correlated data uncertainties. We would like to thank Markus Diehl for useful discussions. The work of C. E. was supported by the Alliance Program of the Helmholtz Association (HA216/EMMI). The work of A. v. M. was supported by the Schweizer Nationalfonds (Grant 200020.124773/1).

A Photon densities

The probability densities $w_{T,L}^{(q)}$ for the virtual photon in (4) are given by

$$w_T^{(q)}(r, Q^2) = \int_0^1 d\alpha \sum_{\lambda, \lambda'} \left| \psi_{\lambda\lambda'}^{(q)T}(\alpha, \mathbf{r}, Q) \right|^2, \quad (28)$$

$$w_L^{(q)}(r, Q^2) = \int_0^1 d\alpha \sum_{\lambda, \lambda'} \left| \psi_{\lambda\lambda'}^{(q)L}(\alpha, \mathbf{r}, Q) \right|^2, \quad (29)$$

where the squared photon wave functions (summed over quark helicities λ, λ') are

$$\sum_{\lambda, \lambda'} \left| \psi_{\lambda\lambda'}^{(q)T}(\alpha, \mathbf{r}, Q) \right|^2 = \frac{3}{2\pi^2} \alpha_{\text{em}} Q_q^2 \{ [\alpha^2 + (1 - \alpha)^2] \epsilon_q^2 [K_1(\epsilon_q r)]^2 + m_q^2 [K_0(\epsilon_q r)]^2 \} \quad (30)$$

and

$$\sum_{\lambda, \lambda'} \left| \psi_{\lambda\lambda'}^{(q)L}(\alpha, \mathbf{r}, Q) \right|^2 = \frac{6}{\pi^2} \alpha_{\text{em}} Q_q^2 Q^2 [\alpha(1 - \alpha)]^2 [K_0(\epsilon_q r)]^2 \quad (31)$$

for transversely and longitudinally polarized photons, respectively. Here $r = \sqrt{\mathbf{r}^2}$ with \mathbf{r} denoting the two-dimensional transverse vector from the antiquark to the quark. Q_q are the quark charges in units of the proton charge, and K_0 and K_1 are modified Bessel functions. The quantity $\epsilon_q = \sqrt{\alpha(1 - \alpha)Q^2 + m_q^2}$ involves the quark mass m_q . For a derivation of the photon wave functions see for example [29].

References

- [1] F. D. Aaron *et al.*, Eur. Phys. J. C **71** (2011) 1579 [arXiv:1012.4355 [hep-ex]].
- [2] O. Nachtmann, *Elementary Particle Physics: Concepts and Phenomena*, Springer Verlag, Berlin, Heidelberg, 1990.
- [3] L. N. Hand, Phys. Rev. **129** (1963) 1834.
- [4] N. N. Nikolaev and B. G. Zakharov, Z. Phys. C **49** (1991) 607.
- [5] N. N. Nikolaev and B. G. Zakharov, Z. Phys. C **53** (1992) 331.
- [6] A. H. Mueller, Nucl. Phys. B **415** (1994) 373.

- [7] K. Golec-Biernat and M. Wüsthoff, Phys. Rev. D **59** (1999) 014017 [arXiv:hep-ph/9807513].
- [8] K. Golec-Biernat and M. Wüsthoff, Phys. Rev. D **60** (1999) 114023 [arXiv:hep-ph/9903358].
- [9] J. Bartels, K. Golec-Biernat and H. Kowalski, Phys. Rev. D **66** (2002) 014001 [arXiv:hep-ph/0203258].
- [10] M. McDermott, L. Frankfurt, V. Guzey and M. Strikman, Eur. Phys. J. C **16** (2000) 641 [arXiv:hep-ph/9912547].
- [11] H. G. Dosch, T. Gousset and H. J. Pirner, Phys. Rev. D **57** (1998) 1666 [arXiv:hep-ph/9707264].
- [12] A. Donnachie and H. G. Dosch, Phys. Rev. D **65** (2002) 014019 [arXiv:hep-ph/0106169].
- [13] A. I. Shoshi, F. D. Steffen and H. J. Pirner, Nucl. Phys. A **709** (2002) 131 [arXiv:hep-ph/0202012].
- [14] E. Iancu, K. Itakura and S. Munier, Phys. Lett. B **590** (2004) 199 [arXiv:hep-ph/0310338].
- [15] J. R. Forshaw, G. Kerley and G. Shaw, Phys. Rev. D **60** (1999) 074012 [arXiv:hep-ph/9903341].
- [16] J. R. Forshaw and G. Shaw, JHEP **0412** (2004) 052 [arXiv:hep-ph/0411337].
- [17] J. R. Forshaw, R. Sandapen and G. Shaw, JHEP **0611** (2006) 025 [arXiv:hep-ph/0608161].
- [18] H. Kowalski and D. Teaney, Phys. Rev. D **68** (2003) 114005 [arXiv:hep-ph/0304189].
- [19] G. Watt and H. Kowalski, Phys. Rev. D **78** (2008) 014016 [arXiv:0712.2670 [hep-ph]].
- [20] L. Motyka, K. Golec-Biernat and G. Watt, in Proceedings of *HERA and the LHC: 4th Workshop on the Implications of HERA for LHC Physics*, Geneva, May 2008, p. 471 [arXiv:0809.4191 [hep-ph]].
- [21] G. Cvetic, D. Schildknecht, B. Surrow and M. Tentyukov, Eur. Phys. J. C **20** (2001) 77 [arXiv:hep-ph/0102229].
- [22] D. Schildknecht, B. Surrow and M. Tentyukov, Phys. Lett. B **499** (2001) 116 [arXiv:hep-ph/0010030].
- [23] M. Kuroda and D. Schildknecht, Phys. Lett. B **618** (2005) 84 [arXiv:hep-ph/0503251].
- [24] M. Kuroda and D. Schildknecht, Phys. Lett. B **670** (2008) 129 [arXiv:0806.0202 [hep-ph]].

- [25] D. Schildknecht, arXiv:1104.0850 [hep-ph].
- [26] M. Kuroda and D. Schildknecht, arXiv:1108.2584 [hep-ph].
- [27] J. L. Albacete, N. Armesto, J. G. Milhano and C. A. Salgado, Phys. Rev. D **80** (2009) 034031 [arXiv:0902.1112 [hep-ph]].
- [28] C. Ewerz and O. Nachtmann, Annals Phys. **322** (2007) 1635 [arXiv:hep-ph/0404254].
- [29] C. Ewerz and O. Nachtmann, Annals Phys. **322** (2007) 1670 [arXiv:hep-ph/0604087].
- [30] C. Ewerz and O. Nachtmann, Phys. Lett. B **648** (2007) 279 [arXiv:hep-ph/0611076].
- [31] C. Ewerz, A. von Manteuffel and O. Nachtmann, Phys. Rev. D **77** (2008) 074022 [arXiv:0708.3455 [hep-ph]].
- [32] C. Ewerz, A. von Manteuffel and O. Nachtmann, JHEP **1103** (2011) 062 [arXiv:1101.0288 [hep-ph]].
- [33] A. Alekhin, J. Blümlein and S. Moch, OPENQCDRAD package, version 1.4 <http://www-zeuthen.desy.de/~alekhin/OPENQCDRAD/>
- [34] P. Jimenez-Delgado and E. Reya, Phys. Rev. D **79** (2009) 074023 [arXiv:0810.4274 [hep-ph]].
- [35] M. Corradi for the H1 and ZEUS Collaborations, in Proceedings of *35th International Conference on High Energy Physics ICHEP 2010*, Paris, July 2010, PoS **ICHEP2010** (2010) 142.
- [36] C. Aidala et al., The EIC Working Group, *A high luminosity, high energy electron-ion-collider - A white paper prepared for the NSAC LRP 2007*, http://web.mit.edu/eicc/DOCUMENTS/EIC_LRP-20070424.pdf
- [37] M. Klein for the LHeC Study Group, in Proceedings of *35th International Conference on High Energy Physics ICHEP 2010*, Paris, July 2010, PoS **ICHEP2010** (2010) 520.